Supplementary Information

Long-range transport of North African dust enhances oceanic iron bioavailability

Site	Fe_T (wt%)	Fe_{HR} (wt%)	Fe_{HR}/Fe_T	Fe_T/Al	$CaCO_3$ (wt%)	TOC (wt%)	Al/Ti	$\delta^{56/54}Fe$ (‰)
658	1.73	0.61	0.36	0.58	62.78	0.64	18.45	-0.06
659	1.76	0.44	0.26	0.52	59.44	0.14	18.16	-0.05
1062	3.86	0.44	0.12	0.54	16.38	0.41	19.24	-0.05
1063	4.29	0.62	0.14	0.56	18.22	0.17	19.56	-0.03

Table S 1: Mean values for all the Fe data at all four sites.

Fe speciation

Fe-extractions from each site are presented in wt%.

658 (n=54)	$Fe_{Na\text{-}Ac}$ (wt%)	Fe_{Dith} (wt%)	Fe_{Ox} (wt%)
>45µm	0.05	0.37	0.20
45µm<x>20µm	0.04	0.37	0.21
<20µm	0.04	0.37	0.20

Table S 2a: Eighteen samples were analyzed for each grain size (total 54 samples).

659 (n=66)	$Fe_{Na\text{-}Ac}$ (wt%)	Fe_{Dith} (wt%)	Fe_{Ox} (wt%)
>45µm	0.04	0.27	0.14
45µm<x>20µm	0.03	0.26	0.14
<20µm	0.03	0.27	0.15

Table S 2b: Twenty-two samples were analyzed for each grain size (total 66 samples).

1062 (n=105)	$Fe_{Na\text{-}Ac}$ (wt%)	Fe_{Dith} (wt%)	Fe_{Ox} (wt%)
>45µm	0.02	0.26	0.17
45µm<x>20µm	0.02	0.26	0.15
<20µm	0.02	0.26	0.15

Table S 2c: Thirty-five samples were analyzed for each grain size (total 105 samples).

1063 (n=159)	$Fe_{Na\text{-}Ac}$ (wt%)	Fe_{Dith} (wt%)	Fe_{Ox} (wt%)
>45µm	0.02	0.38	0.24
45µm<x>20µm	0.02	0.38	0.23
<20µm	0.02	0.37	0.23

Table S 2d: Fifty-three samples were analyzed for each grain size (total 159 samples).

Fe extraction pools in relation to total iron (Fe_T)

658 (n=54)	$Fe_{Na\text{-}Ac}$ % of Fe_T	Fe_{Dith} % of Fe_T	Fe_{Ox} % of Fe_T
>45µm	2.9	21.4	11.6
45µm<x>20µm	2.3	21.6	12.1
<20µm	2.3	21.4	11.3

Table S 3a: Percentage of Fe extracted from Fe_T.

659 (n=66)	$Fe_{Na\text{-}Ac}$ % of Fe_T	Fe_{Dith} % of Fe_T	Fe_{Ox} % of Fe_T
>45µm	2.2	14.8	7.7
45µm<x>20µm	1.6	14.9	7.8
<20µm	2.0	15.8	8.5

Table S 3b: Percentage of Fe extracted from Fe_T.

1062 (n=105)	$Fe_{Na\text{-}Ac}$ % of Fe_T	Fe_{Dith} % of Fe_T	Fe_{Ox} % of Fe_T
>45µm	0.5	8.7	5.4
45µm<x>20µm	0.5	8.8	5.3
<20µm	0.6	8.9	5.5

Table S 3c: Percentage of Fe extracted from Fe_T.

1063 (n=159)	$Fe_{Na\text{-}Ac}$ % of Fe_T	Fe_{Dith} % of Fe_T	Fe_{Ox} % of Fe_T
>45µm	0.5	8.6	5.4
45µm<x>20µm	0.6	9.1	5.9
<20µm	0.6	9.6	6.0

Table S 3d: Percentage of Fe extracted from Fe_T.

Sodium acetate extraction experiment

Sample	$Fe_{Na\text{-}Ac}$ (wt%)	$Fe_{Na\text{-}Ac}$ (%) of Fe_T
Biotite 1	0.15	0.09
Biotite 2	0.17	0.09
Chlorite 1	0.07	0.48
Chlorite 2	0.07	0.52
Fayalite 1	0.10	0.64
Fayalite 2	0.11	0.63
Hornblende 1	0.04	0.23
Hornblende2	0.04	0.20

Table S 4: Percentage of Fe extracted from different minerals by the sodium acetate step. The data indicate that only a very small amount of Fe bound in silicate phases is removed.

Grain Size Distribution (GSD)

METHOD OF MOMENTS		658 (n=18)	659 (n=22)	1062 (n=35)	1063 (n=53)
Arithmetic (µm)	MEAN ($\bar{x}_a$)	41.89	41.43	33.70	32.72
	SKEWNES (Sk_a)	2.04	0.99	1.08	0.97
	KURTOSIS (K_a)	12.67	5.60	5.33	5.04
Geometric (µm)	MEAN ($\bar{x}_g$)	37.49	37.09	29.90	28.76
	SKEWNES (Sk_g)	-0.45	-0.50	-0.23	-0.24
	KURTOSIS (K_g)	3.866	3.32	3.55	3.04
	SIEVING ERROR (%)	8.7	6.3	6.0	7.3

Table S 5: Average GSD (grain size distribution) for all four sites based on dry sieving. Sieving error calculated based on sample loss and comparison with wet sieving.

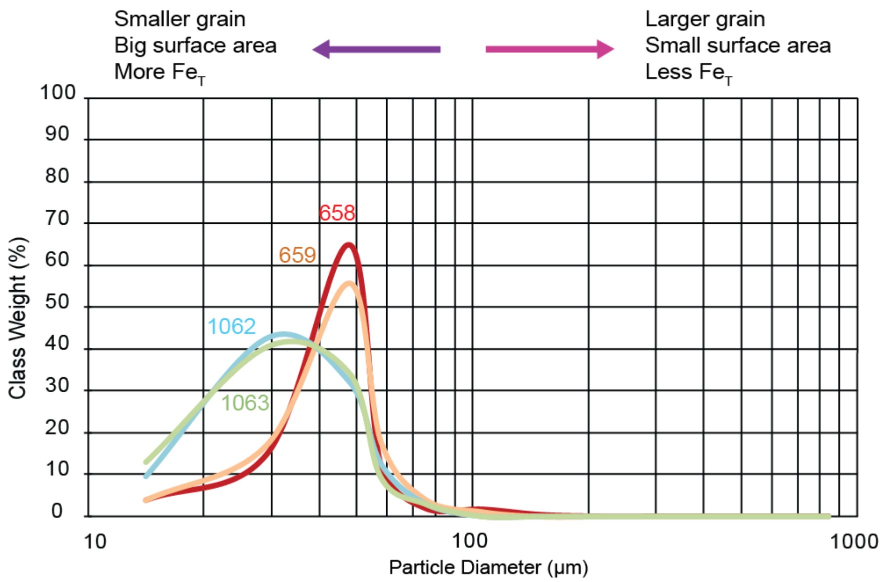

Figure S 1: Plot of grain size data for representative samples from ODP drill cores based on dry sieving.

Export of dust particles in the water column

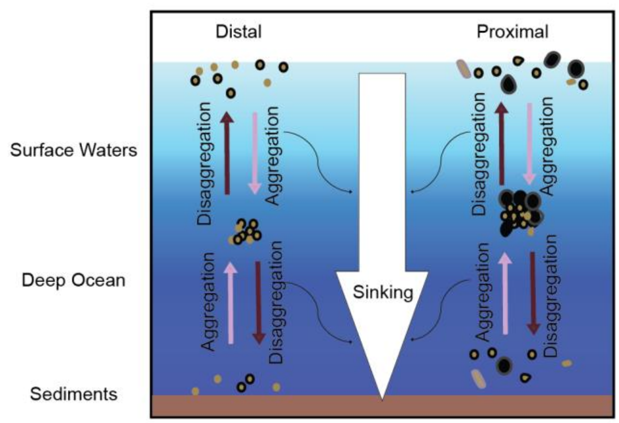

Figure S 2: Schematic representation of hypothesized export of dust particles in the water column. Dust particles can be aggregated into larger, sinking particles, which can sink and be removed from the water column or disaggregate back to slowly settling particles. Dust particles undergo many cycles of aggregation and disaggregation in the water column, making the chemical composition of large aggregates similar to the smaller particles (see text).

Surface area analysis

For a given weight and total volume of a particular material, the surface activity and adsorption volume can vary as a function of the grain size and thus surface area. Surface area is important in our study in terms of reactions during transport that enhance Fe bioavailability.

Surface area can be calculated from the grain size distribution by dividing the size distribution into a finite number of bins and assuming equivalent spherical diameters of particles that correspond to the mean size of each bin (Cepuritis, Garboczi, Ferraris, Jacobsen, & Sørensen, 2017) and using the following relation (Ersahin, Gunal, Kutlu, Yetgin, & Coban, 2006):

$$SA = \frac{6000}{\rho D}, \qquad \text{(Baron \& Willeke, 2001)}$$

where ρ is the material density, and D the size of the particle. We assume a density of 1.49 g/cm^3 for dust (Parnell Jr, Jones, Rutherford, & Goforth, 1986).

	658	659	1062	1063
Arithmetic surface area (m^2/kg)	96.13	97.20	119.49	123.07
Geometric surface area (m^2/kg)	107.41	108.57	134.68	140.02

Table S 6: Surface area calculations based on mean grain size distributions.

Location, average dust deposition fluxes, and age models

Core	Location	Water Depth (m)	Our Estimated Eolian Flux (g m^{-2} y^{-1})	Eolian flux (g m^{-2} y^{-1})	Eolian flux Reference	Age Model Reference
ODP Leg 108 Site 658	21°N, 19°W	2263	20.1	19.2	Adkins et al. (2006); deMenocal et al. (2000)	Tiedemann et al. (1989b)
ODP Leg 108 Site 659	18°N, 21°W	3070	19.5	14.7	Tiedemann et al. (1994)	Tiedemann et al. (1994)
ODP Leg 172 Site 1062	28°N, 74°W	4765	1.5	1.3	Arimoto et al. (2003)	Franz and Tiedemann, (2002); Gruetzner et al (2002)
ODP Leg 172 Site 1063	33°N, 57°W	4585	1.4	1.6	Muhs et al. (2012)	Channell et al. (2012); Gruetzner et al. (2002)

Table S 7: Desert dust deposition (g/m^2/y) estimated from the average of three models (Jickells et al., 2005; Mahowald et al., 2008; Mahowald et al., 1999) representing our best estimate of dust deposition.

Statistical analyses of iron geochemical data for different grain size populations

The normality of the data in each sample was verified by comparing the ANOVA and t-test. The analyses with low p-values (< 0.05) can be considered to have a skewed or non-normal distribution.

The ANOVA test for independent measures is designed to compare the means of three or more independent samples simultaneously of grain size.

SS: Sums of Squares
df: Degree of freedom
MS: Means of squares

The test statistic for testing H_0: $\mu_1 = \mu_2 = ... = \mu_k$ is:

$$F = \frac{\sum N_j(\,\overline{X_j} - \overline{X}\,)\,/\,(k-1)}{\sum\,(X - \overline{X_j}\,)^2\,/(N-k)}$$

The **t test statistic** is used to determine if there is a significant difference between the means of two groups and to determine if they come from the same population.

$$t = \frac{\overline{X_1} - \overline{X_2}}{\sqrt{\left(\frac{(N_1-1)S_1^2 + (N_2-1)S_2^2}{N_1 + N_2 - 2}\right)\left(\frac{1}{N_1} + \frac{1}{N_2}\right)}}$$

Statistical analyses of the Fe_{HR}/Fe_T data for each site

Site 658

	Site 658			
	>45µm	45µm<x>20µm	<20µm	Total
N	18	18	18	54
∑X	6.42	6.42	6.43	19.27
Mean	0.3567	0.3567	0.3572	0.357
$\sum X^2$	2.4	2.4038	2.4149	7.2187
Std.Dev.	0.0805	0.0819	0.0833	0.0803

ANOVA test

Site 658	***SS***	***df***	***MS***	
Between grain sizes	0	2	0	F = 0.00028

Within grain sizes	0.3422	51	0.0067	
Total	0.3422	53		

The *f*-ratio value is 0.00028. The *p*-value is .999724. The result is *not* significant at $p < .05$.

Student´s **T-test** (two-tailed)

	Site 658		
	>45µm vs 45µm<x>20µm	>45µm vs <20µm	45µm<x>20µm vs <20µm
t-value	0	-0.02018	0.02035
p-value	1	0.984019	0.983887
Significance at $p <$ 0.05	*not* significant	*not* significant	*not* significant

Table S 8a: Results of statistical analysis. ANOVA and T-test for site 658 that are significant at the P< 0.05 level are colored in black and are not significant when red.

Site 659

	Site 659			
	>45µm	45µm<x>20µm	<20µm	Total
N	22	22	22	66
$\sum X$	5.43	5.43	5.8	16.66
Mean	0.2468	0.2468	0.2636	0.252
$\sum X^2$	1.3621	1.4161	1.547	4.3252
Std.Dev.	0.0323	0.0601	0.0292	0.0429

ANOVA test

Site 659	***SS***	***df***	***MS***	
Between grain sizes	0.0041	2	0.0021	F = 1.1298
Within grain sizes	0.1157	63	0.0018	
Total	0.1198	65		

The *f*-ratio value is 1.1298. The *p*-value is .329554. The result is *not* significant at $p < .05$.

Student´s **T-test (**two-tailed)

	Site 659		
	>45µm vs 45µm<x>20µm	>45µm vs <20µm	45µm<x>20µm vs <20µm
t-value	0	-1.81231	-1.1804
p-value	1	0.077091	0.244482
Significance at $p <$ 0.05	*not* significant	*not* significant	*not* significant

Table S 8b: Results of statistical analysis. ANOVA and T-test for site 659 that are significant at the P< 0.05 level are colored in black and are not significant when red.

Site 1062

	Site 1062			
	>45µm	45µm<x>20µm	<20µm	Total
N	35	35	35	105
∑X	4.09	3.78	4.21	12.08
Mean	0.1169	0.108	0.1203	0.115
$\sum X^2$	0.5139	0.448	0.5583	1.5202
Std.Dev.	0.0325	0.0342	0.0391	0.0354

ANOVA test

Site 1062	***SS***	***df***	***MS***	
Between grain sizes	0.0028	2	0.0014	F = 1.12435
Within grain sizes	0.1276	102	0.0013	
Total	0.1304	104		

The *f*-ratio value is 1.12435. The *p*-value is .328856. The result is *not* significant at $p < .05$.

Student´s **T-test (**two-tailed)

	Site 1062		
	>45µm vs 45µm<x>20µm	>45µm vs <20µm	45µm<x>20µm vs <20µm
t-value	1.1104	-0.39904	-1.39988

p-value	0.270739	0.691117	0.083048
Significance at $p < 0.05$	*not* significant	*not* significant	*not* significant

Table S 8c: Results of statistical analysis. ANOVA and T-test for site 1062 that are significant at the P< 0.05 level are colored in black and are not significant when red.

Site 1063

	Site 1063			
	>45µm	45µm<x>20µm	<20µm	Total
N	53	53	53	159
∑X	7.67	7.63	7.99	23.29
Mean	0.1447	0.144	0.1508	0.146
$\sum X^2$	1.1435	1.1355	1.2499	3.5289
Std.Dev.	0.0254	0.0267	0.0295	0.0273

ANOVA test

Site1063	***SS***	***df***	***MS***	
Between grain sizes	0.0015	2	0.0007	F = 0.98825
Within grain sizes	0.116	156	0.0007	
Total	0.1174	158		

The *f*-ratio value is 0.98825. The *p*-value is .374545. The result is *not* significant at $p < .05$.

Student´s **T-test (**two-tailed)

	Site 1063		
	>45µm vs 45µm<x>20µm	>45µm vs <20µm	45µm<x>20µm vs <20µm
t-value	0.14913	-1.1285	-1.24195
p-value	0.881742	0.261706	0.217049
Significance at $p < 0.05$	*not* significant	*not* significant	*not* significant

Table S 8d: Results of statistical analysis. ANOVA and T-test for site 1063 that are significant at the P< 0.05 level are colored in black and not significant in red.

Statistical analyses of GDS during glacial-interglacial periods

The one sample *t*-Test is used to determine the difference between a sample mean and a known value of the mean in the population to check for the variability of grain size distribution during glacial-interglacial time periods.

The null hypothesis is:

H_o: M-µ = 0, where M is the sample mean and µis the population mean or hypothesized mean.

$$t = \frac{M - \mu}{\sqrt{\left(\frac{\sum X^2 - ((\sum X)^2/N)}{(N-1)(N)}\right)}}$$

T-test	658 (n=18)	659 (n=22)	1062 (n=35)	1063 (n=53)
t-value	-0.15	-0.30	-0.35	-1.33
p-value	0.88	0.76	0.72	0.19
Significance at $p < 0.05$	*not* significant	*not* significant	*not* significant	*not* significant

Table S 9: Results of statistical analysis. T-test for all four sites that are significant at the $p< 0.05$ level are colored in black and are not significant when red.

Geochemical analysis T- test during glacial-interglacial periods

We used a single sample t-test to determine whether our samples show significant variations of Fe distribution during glacial and interglacial periods.

Site 658	*t*-value	p-value	significance at $p < .05$
Fe_T	-0.037	0.970	*not* significant
Fe_{HR}/Fe_T	-0.176	0.863	*not* significant
TOC	0.089	0.930	*not* significant

Table S 10a: Results of statistical analysis for site 658.

Site 659	*t*-value	p-value	significance at $p < .05$
Fe_T	0.009	0.993	*not* significant
Fe_{HR}/Fe_T	0.462	0.649	*not* significant
TOC	0.162	0. 873	*not* significant

Table S 10b: Results of statistical analysis for site 659.

Site 1062	*t*-value	p-value	significance at $p < .05$
Fe_T	0.013	0.980	*not* significant
Fe_{HR}/Fe_T	-0.572	0.571	*not* significant
TOC	0.049	0.962	*not* significant

Table S 10c: Results of statistical analysis for site 1062.

Site 1063	*t*-value	p-value	significance at *p* < .05
Fe_T	2.714	0.009	significant
Fe_{HR}/Fe_T	1.353	0.182	*not* significant
TOC	-0.107	0.182	*not* significant

Table S 10d: Results of statistical analysis for site 1063.

Fe Isotope Samples Numbers

Site	Total number of Samples	$\delta^{56/54}$Fe (‰)
658	10	-0.06
659	8	-0.05
1062	10	-0.05
1063	10	-0.03

Table S 11: Fe isotopes were measured from all four sites, resulting in a total of 38 analyses across various grain sizes.

Daily Aerosol Optical Depth

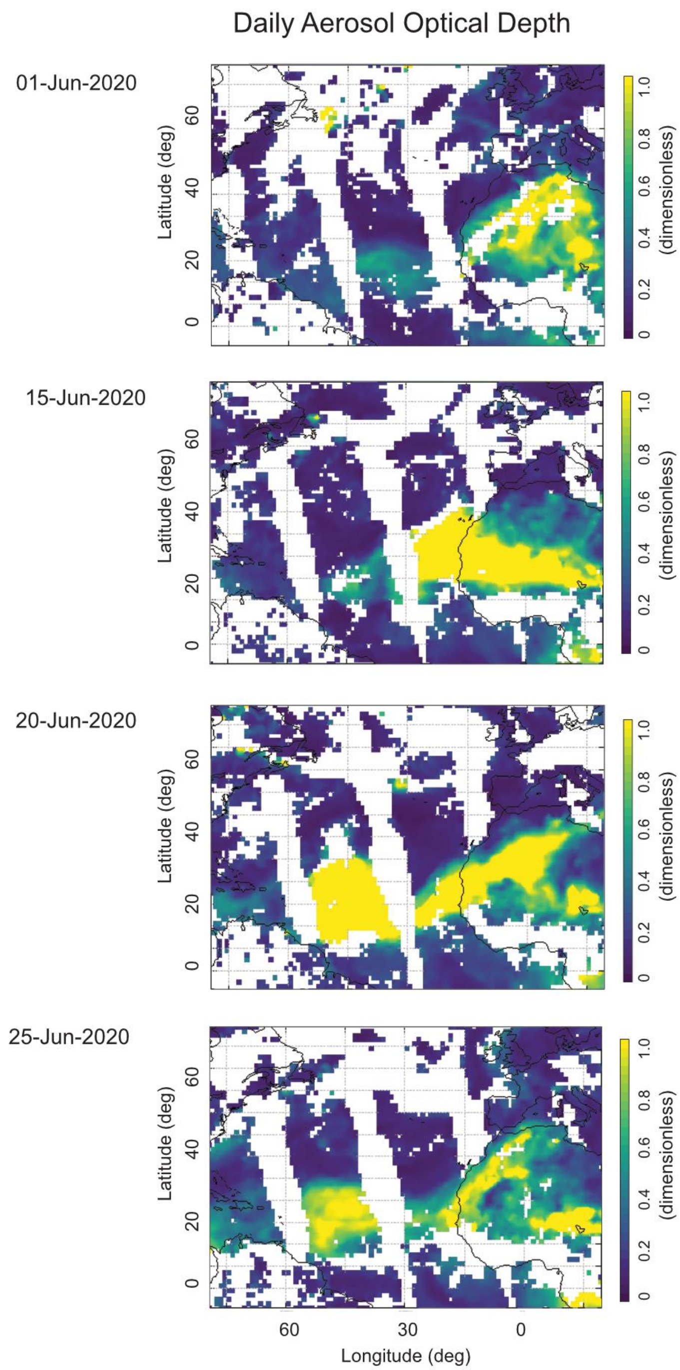

Figure S3: Daily Aerosol Optical Depth from VIIRS - Visible Infrared Imaging Radiometer Suite (https://earthdata.nasa.gov/earth-observation-data/near-real-time/download-nrt-data/viirs-nrt)

Modern Seasonal Distribution of Aerosol Optical Depth and Chlorophyll Concentration

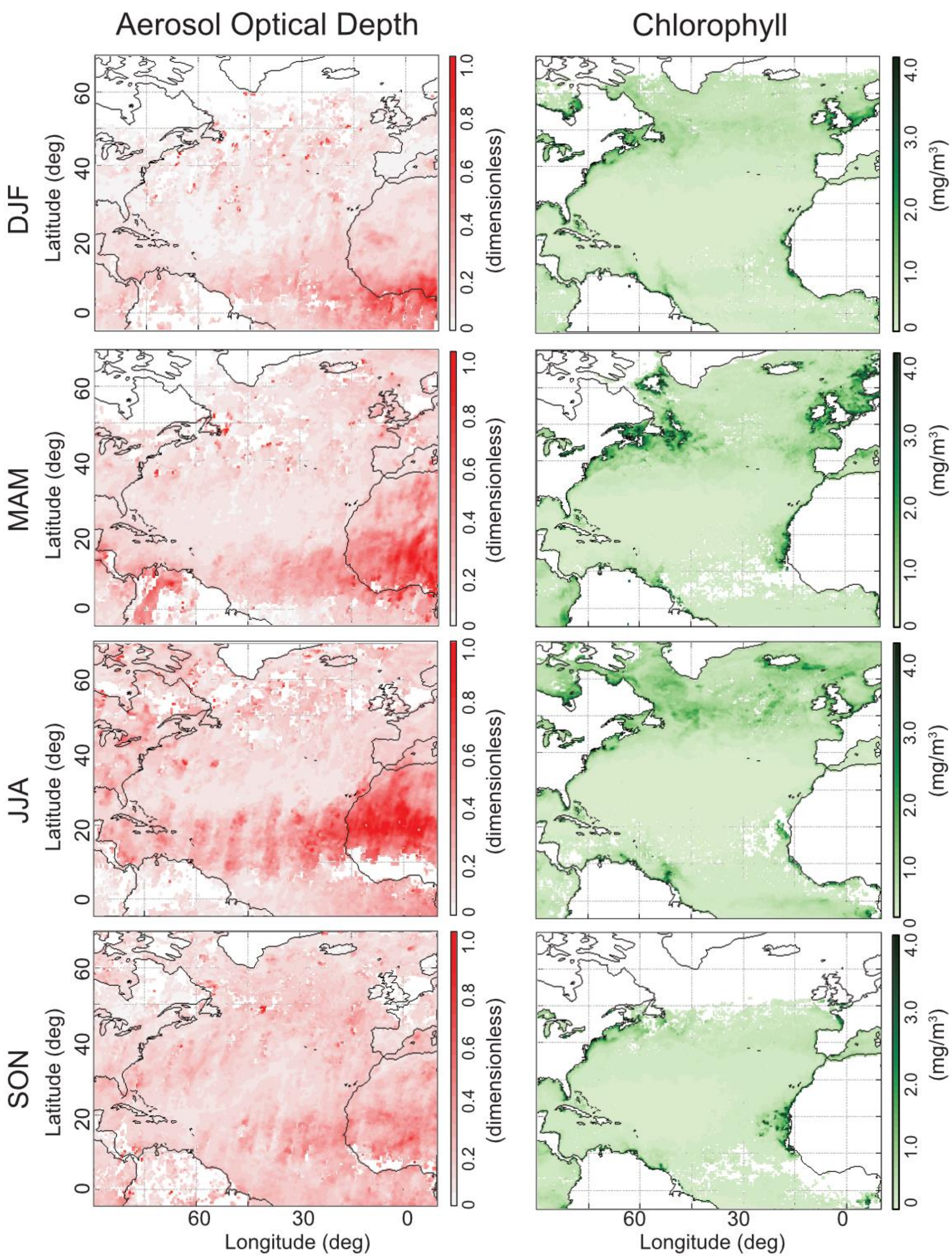

Figure S4: Seasonal (DJF, MAM, JJA and SON) aerosol optical depth (550nm) and Chlorophyll average concentration between 2009-2019 over the North Atlantic Ocean. Aerosol optical depth data source is from MIRS – Multi-angle Imaging SpectroRadiometer (https://misr.jpl.nasa.gov/getData/accessData/)
Chlorophyll data source is from MODIS – Moderate Resolution Imaging Spectrometer (https://modis.gsfc.nasa.gov/data/)

Linear Regression Analysis Model

For hypothesis testing of the variability of spatial Fe distribution we use linear regression model. Our goal is to explore the relationship between p-values and confidence intervals for linear regression parameters. The Fit output is used to estimate p-values using the tcdf function and confidence intervals using the tinv function.

1. In relationship to distance
   The distance is an approximate estimate calculated based on longitude and latitude points using the Longitude/latitude distance calculator from NOAA (https://www.nhc.noaa.gov/gccalc.shtml) and is expressed in kilometers (km),

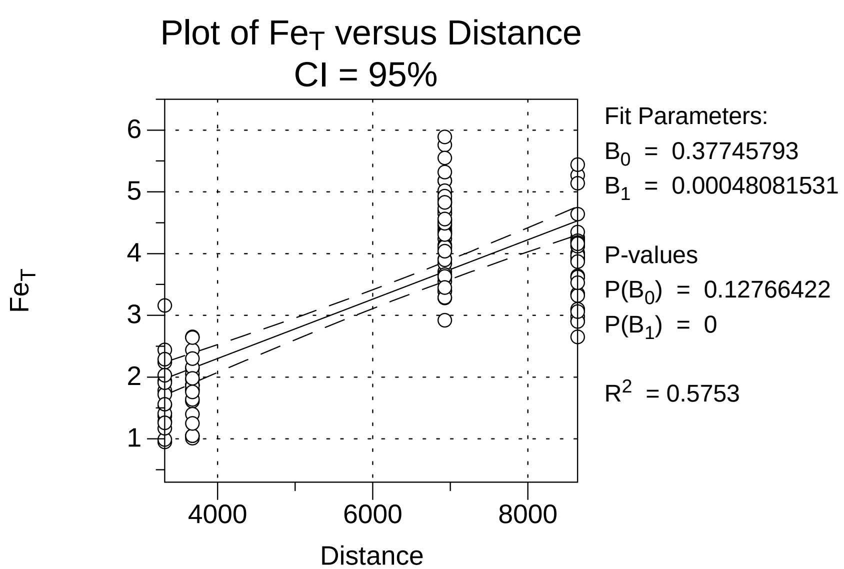

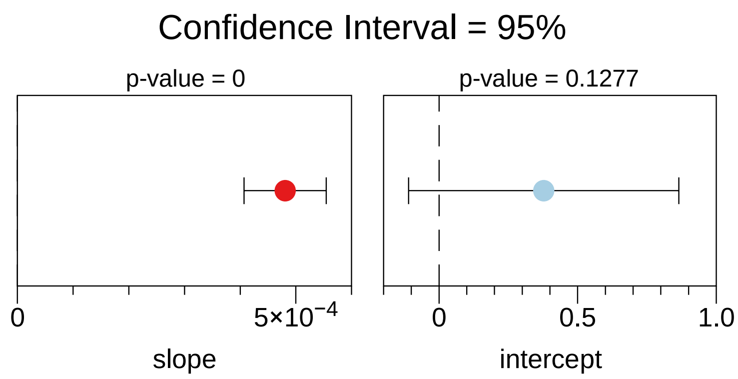

Figure S 5a: Fe_T versus Distance

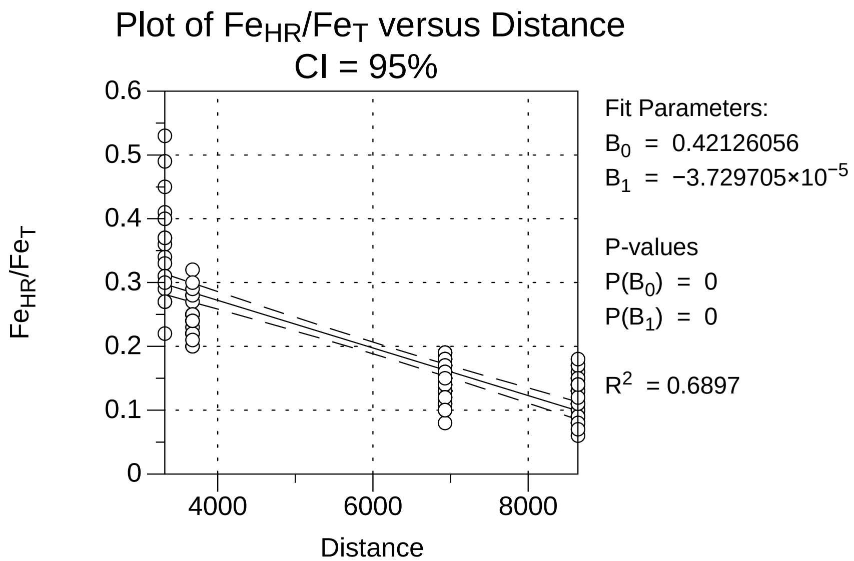

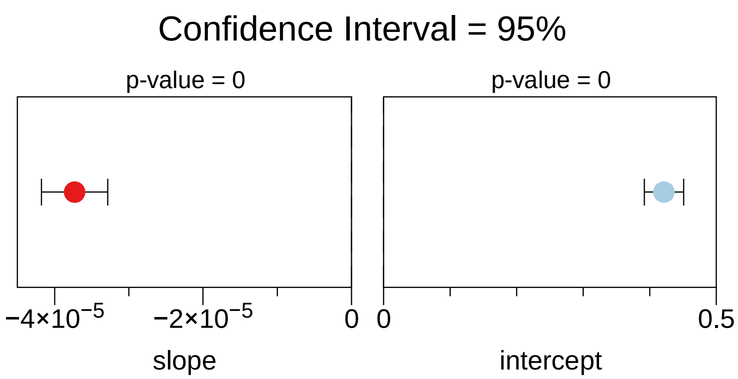

Figure S 5b: Linear regression of Fe_{HR}/Fe_T versus Distance

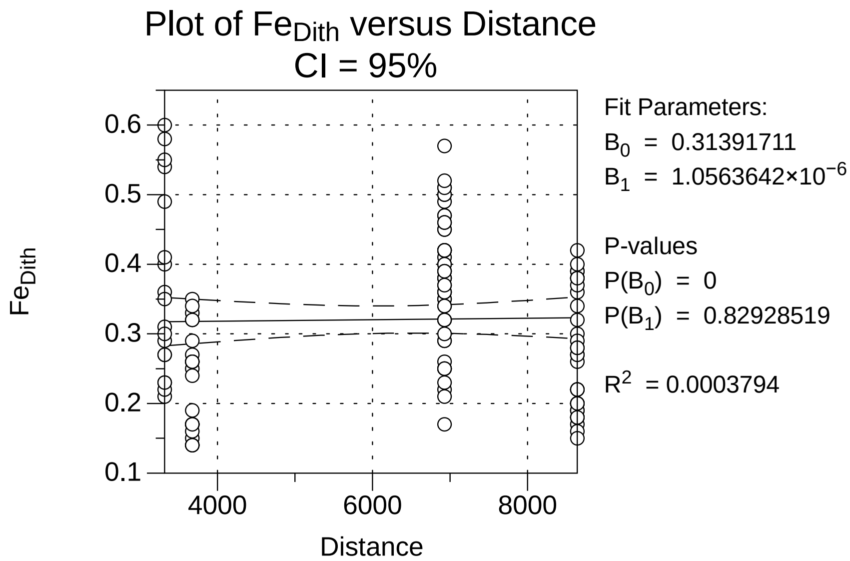

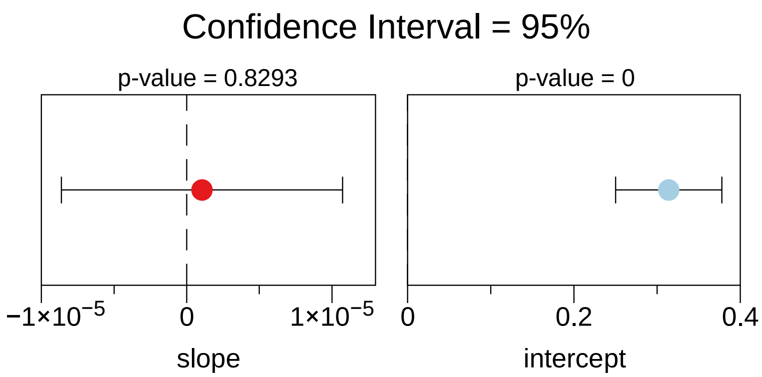

Figure S 5c: Linear regression of $Fe_{Dith\ versus}$ Distance

2. In relationship to $CaCO_3$

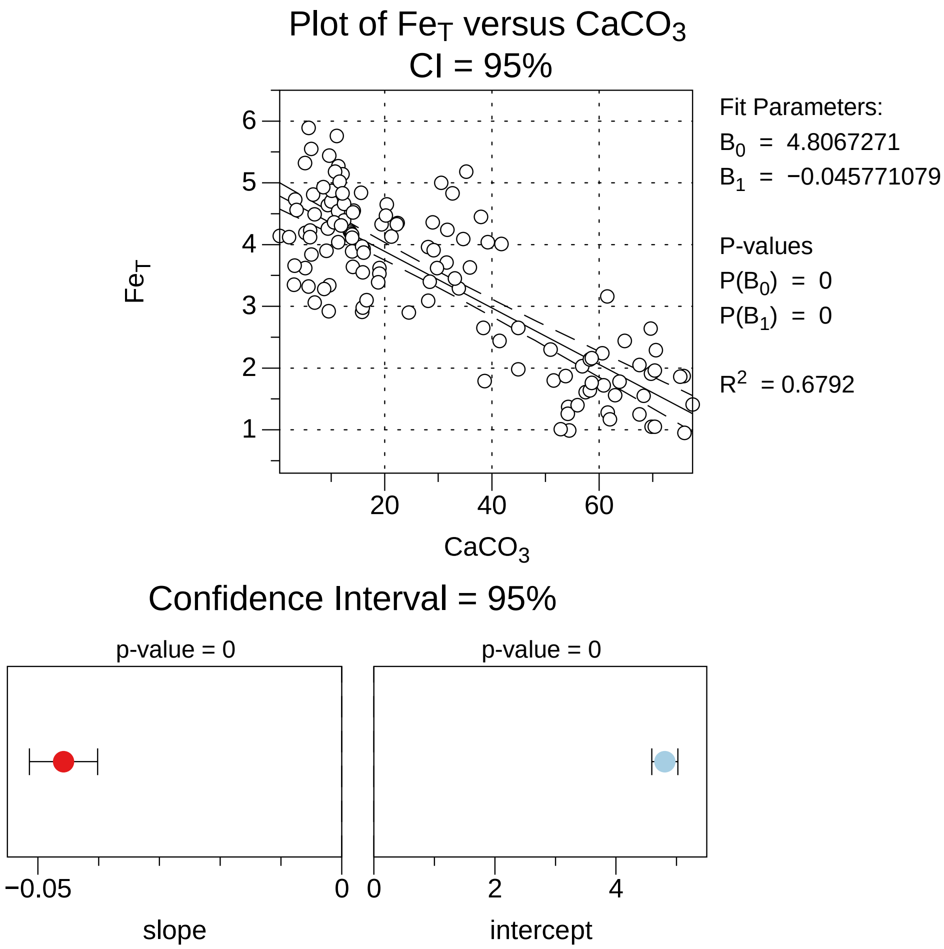

Figure S 6a: Linear regression of Fe_T versus $CaCO_3$

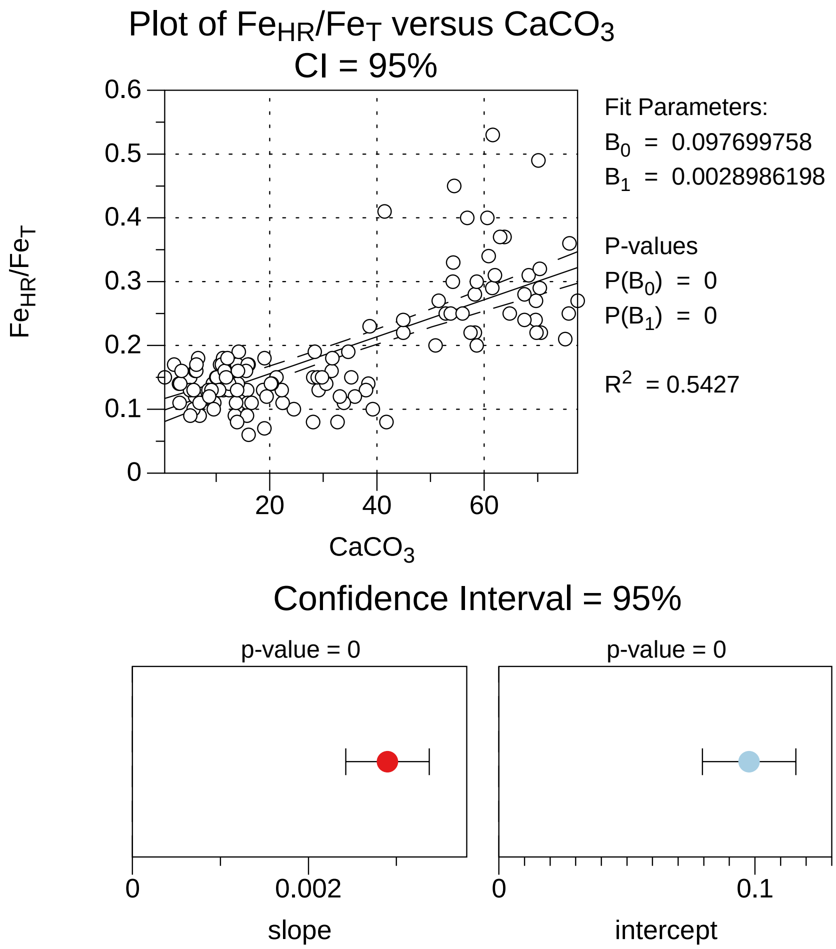

Figure S 6b: Linear regression of Fe_{HR}/Fe_{T} versus $CaCO_3$

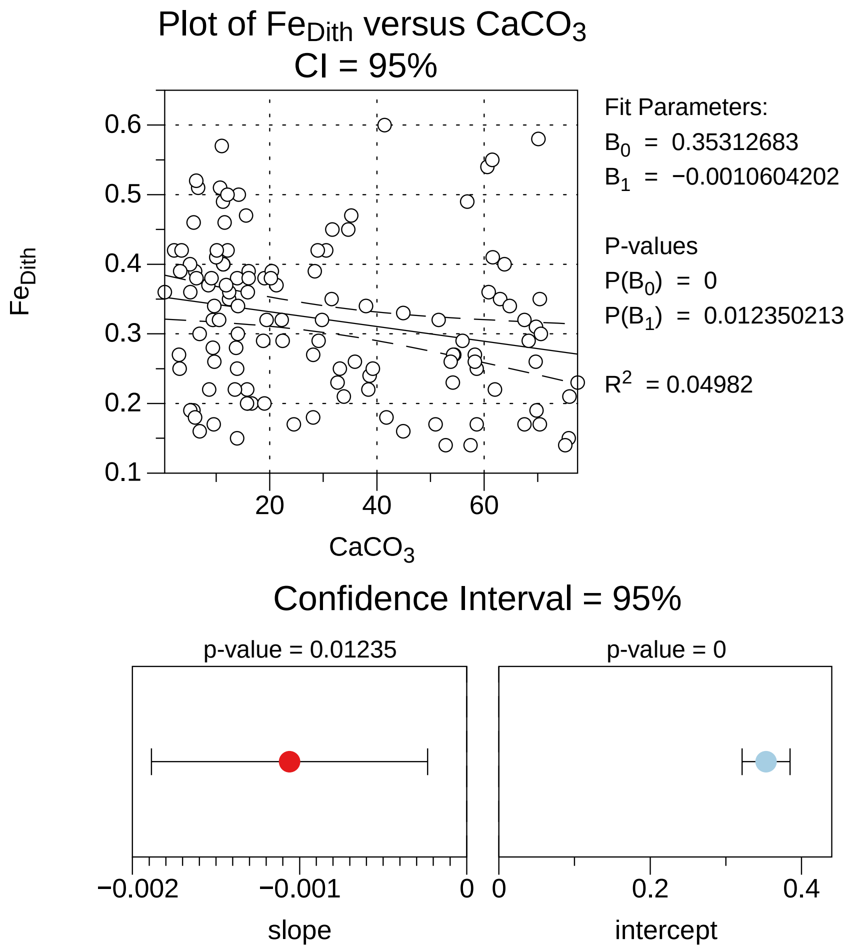

Figure S 6c: Linear regression of Fe_{Dith} versus $CaCO_3$

c-Genie Earth Model

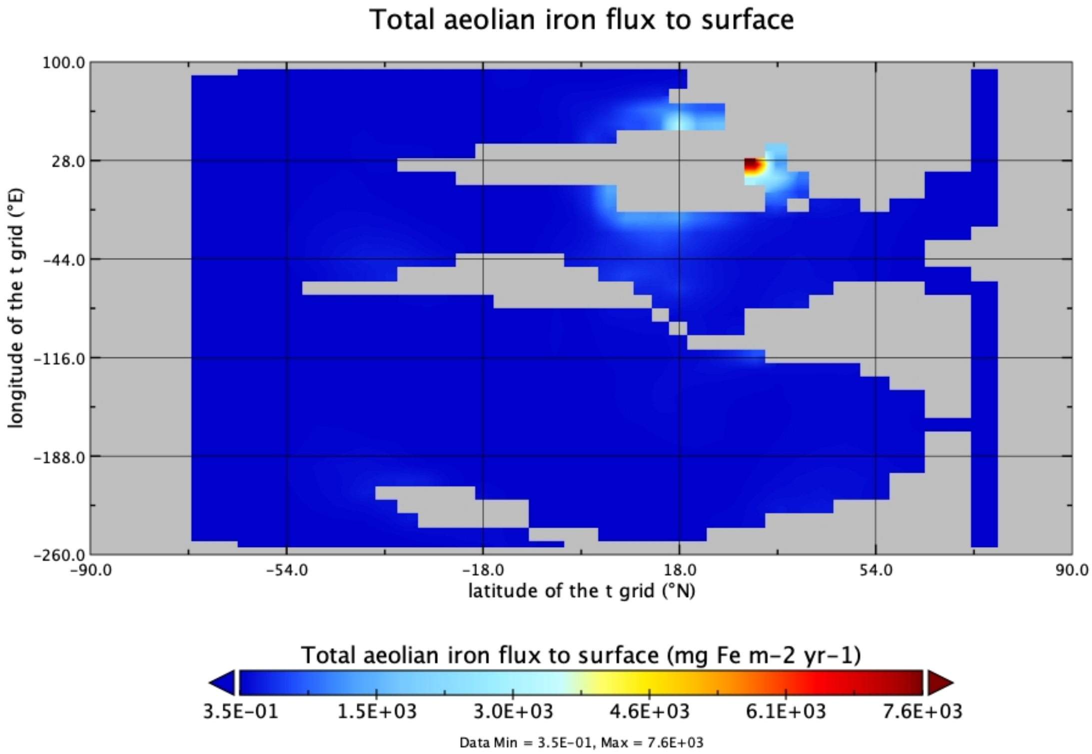

Figure S 7a. Total delivery of aeolian Fe flux to the surface ocean.

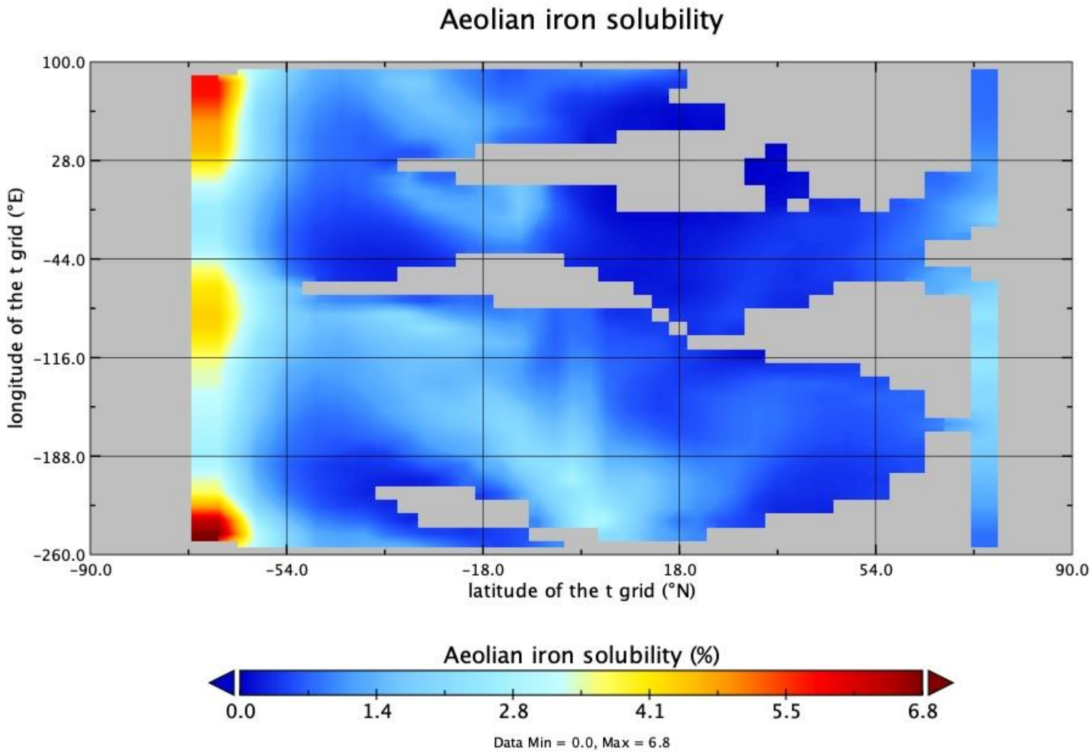

Figure S 7b: Bust-borne Fe solubility distribution.

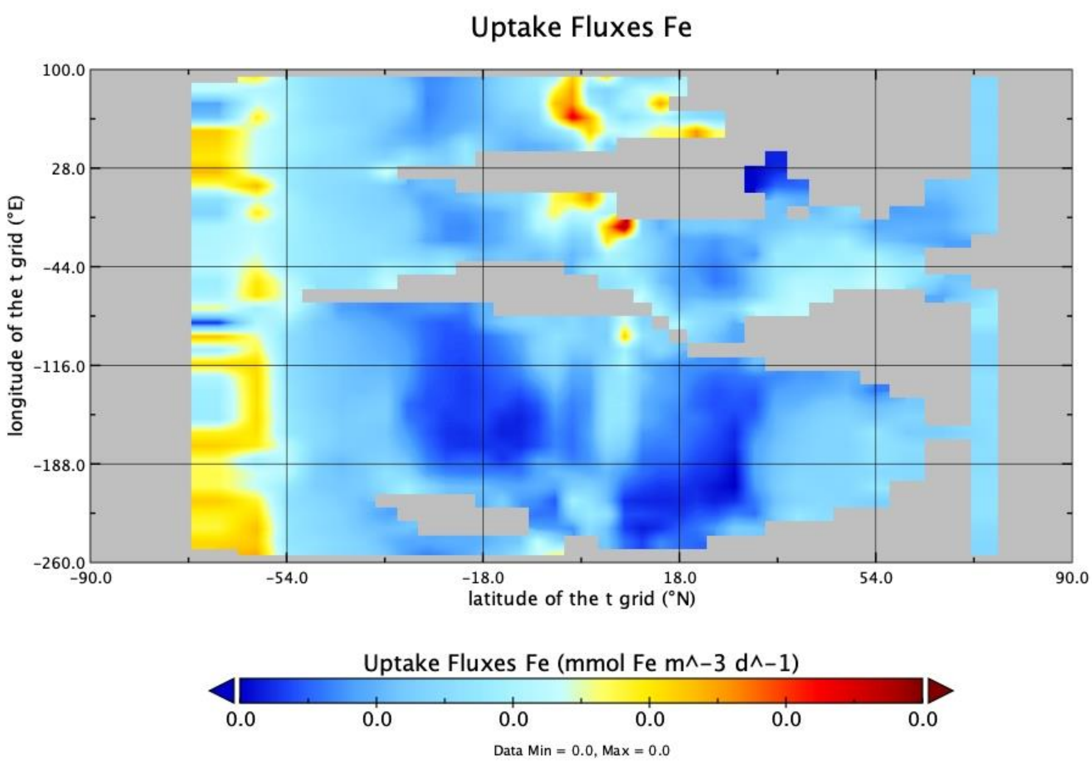

Figure S 7c: Uptake of Fe by the primary producers.

References

Baron, P. A., & Willeke, K. (2001). Aerosol measurement: principles, techniques, and applications.

Cepuritis, R., Garboczi, E. J., Ferraris, C. F., Jacobsen, S., & Sørensen, B. E. (2017). Measurement of particle size distribution and specific surface area for crushed concrete aggregate fines. *Advanced Powder Technology, 28*(3), 706-720.

Ersahin, S., Gunal, H., Kutlu, T., Yetgin, B., & Coban, S. (2006). Estimating specific surface area and cation exchange capacity in soils using fractal dimension of particle-size distribution. *Geoderma, 136*(3-4), 588-597.

Jickells, T. D., An, Z. S., Andersen, K. K., Baker, A. R., Bergametti, G., Brooks, N., . . . Torres, R. (2005). Global iron connections between desert dust, ocean biogeochemistry, and climate. *Science, 308*(5718), 67-71. doi:DOI 10.1126/science.1105959

Mahowald, N., Jickells, T. D., Baker, A. R., Artaxo, P., Benitez-Nelson, C. R., Bergametti, G., . . . Tsukuda, S. (2008). Global distribution of atmospheric phosphorus sources, concentrations and deposition rates, and anthropogenic impacts. *Global biogeochemical cycles, 22*(4). doi:Artn Gb402610.1029/2008gb003240

Mahowald, N., Kohfeld, K., Hansson, M., Balkanski, Y., Harrison, S. P., Prentice, I. C., . . . Rodhe, H. (1999). Dust sources and deposition during the last glacial maximum and current climate: A comparison of model results with paleodata from ice cores and marine sediments. *Journal of Geophysical Research-Atmospheres, 104*(D13), 15895-15916. doi:Doi 10.1029/1999jd900084

Parnell Jr, C. B., Jones, D. D., Rutherford, R. D., & Goforth, K. J. (1986). Physical properties of five grain dust types. *Environmental Health Perspectives, 66*, 183-188.